

Supporting Information

Star Polymer Synthesis via λ -Orthogonal Photochemistry**

Kai Hildebrandt, Michael Kaupp, Edgar Molle, Jan P. Menzel, James P. Blinco, and
Christopher Barner-Kowollik**

Materials

Acetic acid (glacial, $\geq 99.85\%$), acetone (ACS grade, VWR), acetonitrile (99.9%, Fisher Scientific), aluminium chloride (99%, Acros), aniline (99%, Sigma-Aldrich), copper(I) chloride (99.99%, Sigma-Aldrich), copper sulfate pentahydrate (98%, Acros), 18-crown-6 (99%, Acros), dichloromethane (DCM, HPLC grade, Acros), dichloromethane (DCM, 99.8%, extra dry, Acros), 1-(3-dimethylaminopropyl)-3-ethylcarbodiimide hydrochloride (EDC, 98+%, Acros), 4-dimethylaminopyridine (DMAP, 99%, abcr), 2,3-dimethylanisole (97%, Sigma-Aldrich), ethanol (99.8%, VWR), ethyl acetate (99.5%, VWR), 4-formyl benzoic acid (96%, Acros), furan (98%, Sigma-Aldrich), hexylamine (98%, Merck), hydrochloric acid (37%, Roth), magnesium sulfate ($\geq 99\%$, Roth), maleic anhydride ($\geq 99\%$, Sigma-Aldrich), maleimide (98+%, VWR), methanol (99.9%, VWR), methyl 4-(bromomethyl)benzoate (97%, TCI), n-hexane (99%, VWR), N,N,N',N',N''-pentamethyldiethylenetriamine (PMDTA, 99+ %, Acros), o-(2-azidoethyl)nonadecaethylene glycol (HO-PEG₁₉-N₃, $\geq 95\%$, Sigma-Aldrich), petroleum ether (ACS reagent, Sigma-Aldrich), poly(L-lactide) N-2-hydroxyethylmaleimide terminated (pL, $M_n \approx 5200 \text{ g}\cdot\text{mol}^{-1}$, Sigma-Aldrich), potassium carbonate (99%, Alfa Aesar), potassium peroxodisulfate (99%, Merck), propargyl alcohol (99 %, abcr), p-toluenesulfonyl hydrazide (99%, Merck), pyridine (99%, Alfa Aesar), sodium nitrite ($\geq 97\%$, Sigma-Aldrich), tetrahydrofuran (THF, 99.85%, extra dry, Acros), toluene (99%, Alfa Aesar), tris(2-aminoethyl)amine (96%, Sigma-Aldrich) were used as received.

4-((2-formyl-3-methylphenoxy)methyl) benzoic acid was synthesised according to the literature.^[1]

Characterization

^1H NMR spectroscopy was performed using a Bruker Ascend 400 at 400 MHz. All samples were dissolved in deuterated acetonitrile or CDCl_3 . The δ -scale is referenced to the internal standard tetramethylsilane (TMS, $\delta = 0.00$ ppm).

ESI-MS (Electrospray Ionization Mass Spectrometry) spectra were recorded on a Q Exactive (Orbitrap) mass spectrometer (ThermoFisher Scientific, San Jose, CA, USA) equipped with an HESI II probe. The instrument was calibrated in the m/z range of 74-1822 using a premixed standard comprising caffeine, Met-Arg-Phe-Ala acetate (MRFA), and a mixture of fluorinated phosphazenes (Ultramark 1621). A constant spray voltage of 4.6 kV and a dimensionless sweep gas flow rate of 5 were applied. The capillary temperature and the S-lens RF level were set to 320 °C and 62.0, respectively. The samples were dissolved with a concentration of 0.05 $\text{mg}\cdot\text{mL}^{-1}$ in a mixture of THF and MeOH (3:2) containing 100 μmol sodium trifluoroacetate (NaTFA). The samples were infused with a flow of 5 $\mu\text{L}\cdot\text{min}^{-1}$.

Gel Permeation Chromatography (GPC) measurements were performed on a Polymer Laboratories (Varian) PL-GPC 50 Plus Integrated System, comprising an autosampler, a PLgel 5 mm bead-size guard column (50 x 7.5 mm), one PLgel 5mm Mixed E column (300 x 7.5 mm), three PLgel 5mm Mixed C columns (300 x 7.5 mm) and a differential refractive index detector using THF as the eluent at 35 °C with a flow rate of 1 $\text{mL}\cdot\text{min}^{-1}$. The present GPC system was calibrated using linear poly(styrene) standards ranging from 476 to $2.5\cdot 10^6$ $\text{g}\cdot\text{mol}^{-1}$ and linear poly(methyl methacrylate) standards ranging from 700 to $2\cdot 10^6$ $\text{g}\cdot\text{mol}^{-1}$. The resulting molar mass distributions were determined by universal calibration using Mark-Houwink parameters for polystyrene ($K = 14.1\cdot 10^{-5}$ $\text{dL}\cdot\text{g}^{-1}$, $\alpha = 0.7$).

UV/vis spectra were recorded in dichloromethane on a Varian Cary 300 Bio spectrophotometer.

Irradiation

The samples to be irradiated were placed on a metallic disc revolving around a compact low-pressure fluorescent lamp (Cleo PL-L, Philips Deutschland GmbH) emitting at 365 nm (± 50 nm, 36 W), a compact low-pressure fluorescent lamp (Arimed B6, Cosmedico GmbH) emitting at 340 nm (± 60 nm, 36 W) at a distance of 40-50 mm in a custom built photoreactor (Figure S2). No bandpass filter was used for the irradiations.

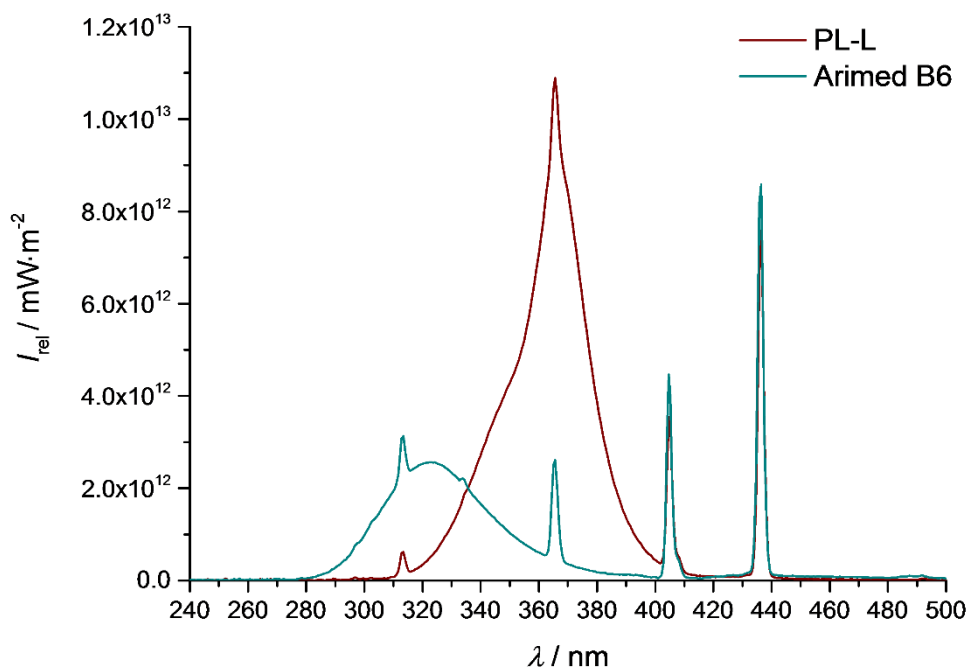


Figure S1. Emission spectra of the two employed compact low-pressure fluorescent lamps PL-L (36 W) and Arimed B6 (36 W). The emission spectra were recorded with a UV sensor (Opsytec Dr. Gröbel GmbH; Ettlingen, Germany).

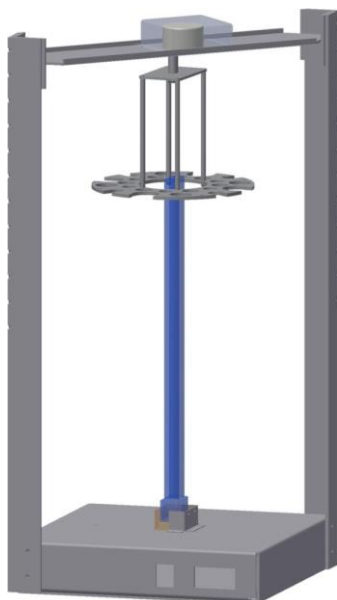
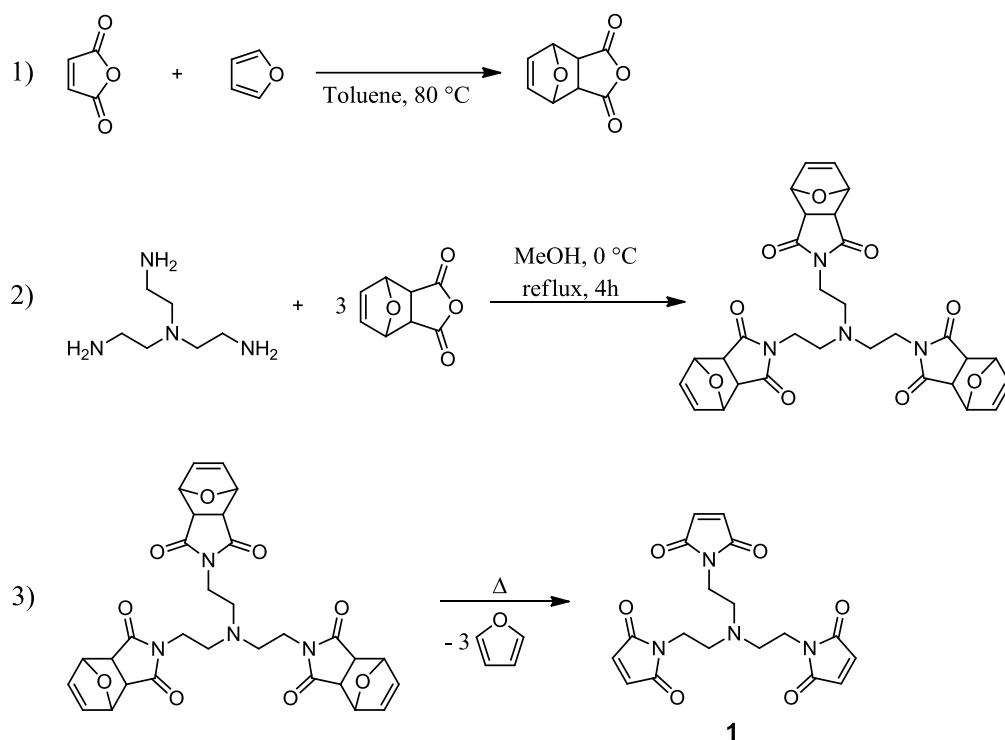


Figure S2. Drawing of the custom-built photoreactor employed in the current study. The angular velocity is 0.5 rad s^{-1} .

Synthesis

Tris(2-maleimidoethyl)amine 1



Step 1: 30.0 g (306 mmol, 1 eq.) of maleic anhydride was suspended in 150 mL toluene and the mixture was heated to 80 °C. 33.4 mL (459 mmol, 1.5 eq.) furan was added and the turbid solution was stirred for 6 h. The mixture was subsequently cooled to ambient temperature. After 1 h, the resulting white crystals were collected by filtration and washed with 60 mL petroleum ether in order to obtain 44.4 g (87 % yield) of the product as small white needles.

Step 2: 5.7 g (34 mmol, 5 eq.) of the product obtained in Step 1 was dissolved in 150 mL methanol and the solution was cooled to 0 °C. A solution of 1.0 g tris(2-aminoethyl)amine in 50 mL methanol was added dropwise to the reaction mixture within 30 min. The solution was stirred at 0 °C for 5 min, 30 min at ambient temperature and the solution was then refluxed for 4 h. After this time, the yellow solution was concentrated to ca. 75 mL and left to crystallize at 4 °C overnight. The obtained pale yellow crystals were filtered and washed with ethyl acetate. Residual solvent was evaporated under reduced pressure. Yield: 945 mg (24 %).

Step 3: 3.0 g (5.1 mmol, 1 eq.) of product 2 was dissolved in 60 mL toluene and the solution was refluxed for 7 h. The solvent was removed subsequently under reduced pressure. The residual solid was dissolved in ethyl acetate and underwent flash chromatography (dichloromethane/ethyl acetate 60/40). Yield: 1.56 g (84 %).

$^1\text{H NMR}$ (CDCl_3) δ /ppm 2.64 (t, $^3\text{J} = 6.6$ Hz, 6H), 3.45 (t, $^3\text{J} = 6.6$ Hz, 6H), 6.61 (s, 6H).

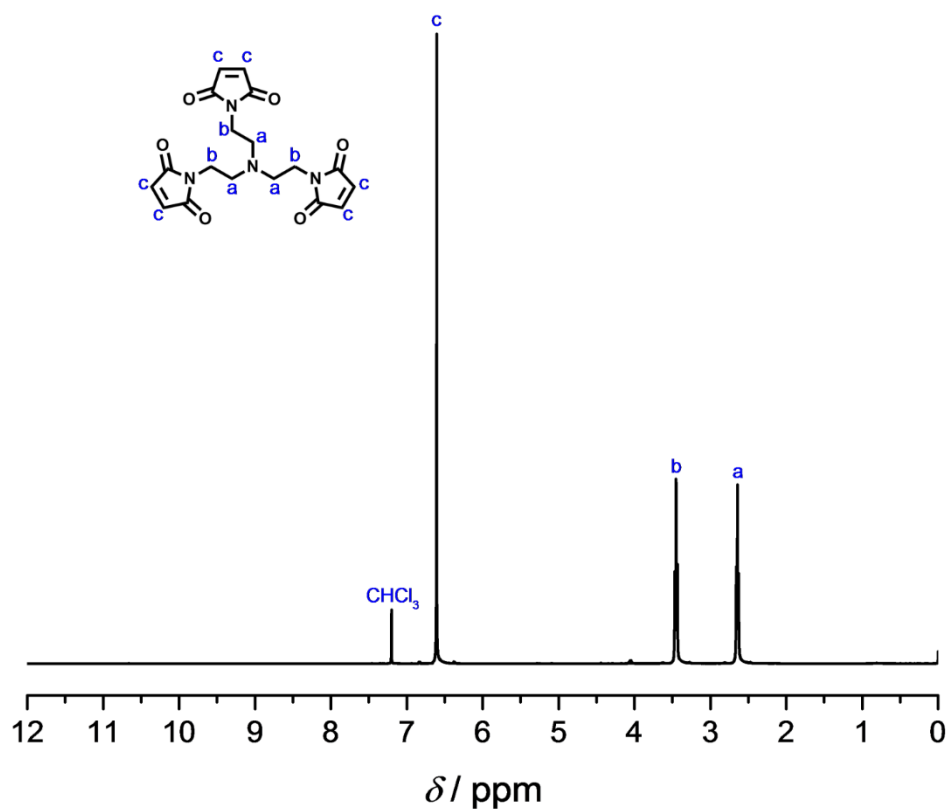
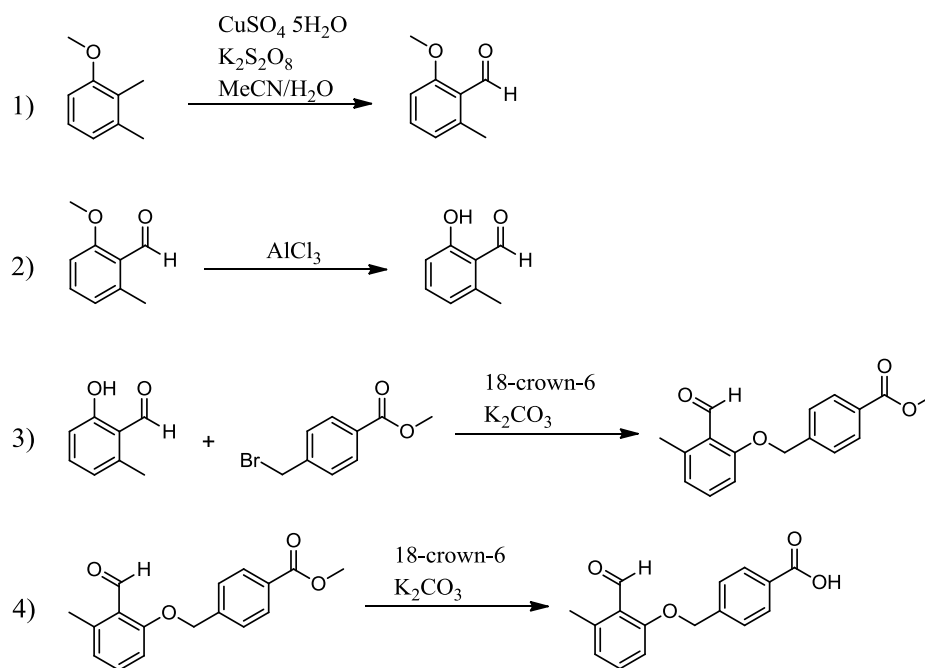


Figure S3. ^1H NMR of tris(2-maleimidoethyl)amine in CDCl_3 .

4-((2-formyl-3-methylphenoxy)methyl) benzoic acid



The synthesis of 4-((2-formyl-3-methylphenoxy)methyl) benzoic acid was performed in four steps according to the appropriate literature procedures: step 1,^[2] step 2,^[3] step 3,^[2] and step 4.^[1] The purity of **5** was confirmed by ¹H NMR.^[1]

¹H NMR (DMSO-d₆) δ/ppm 2.47 (s, 3H), 5.34 (s, 2H), 6.89 (d, ³J = 7.6 Hz, 1H), 7.13 (d, ³J = 8.4 Hz, 1H), 7.47 (t, ³J = 7.9 Hz, 1H), 7.60 (d, ³J = 8.4 Hz, 1H), 7.97 (d, ³J = 8.4 Hz, 1H), 10.62 (s, 1H), 12.97 (s, 1H).

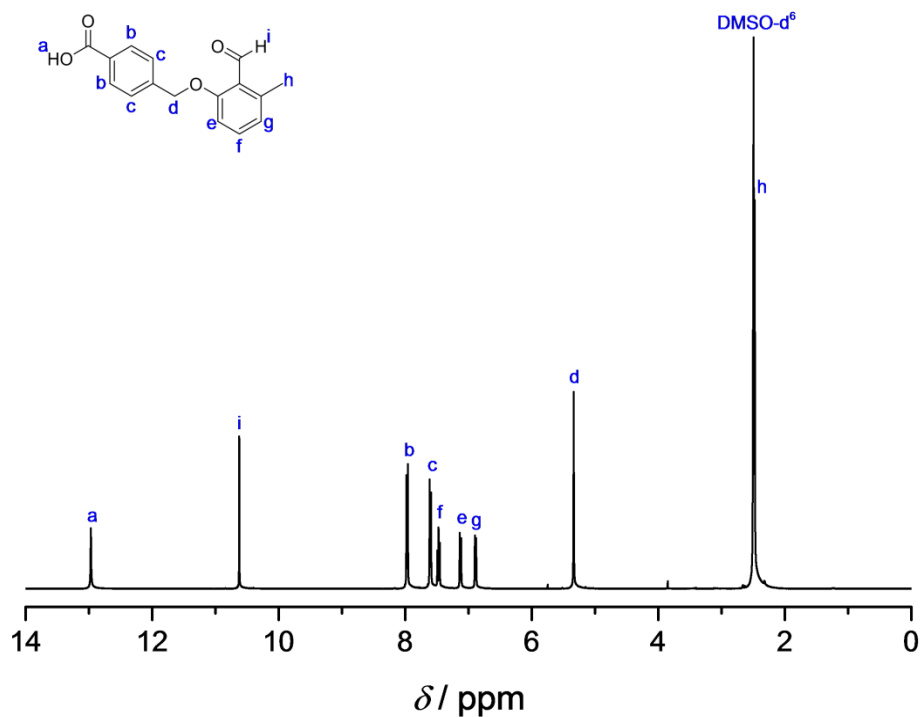
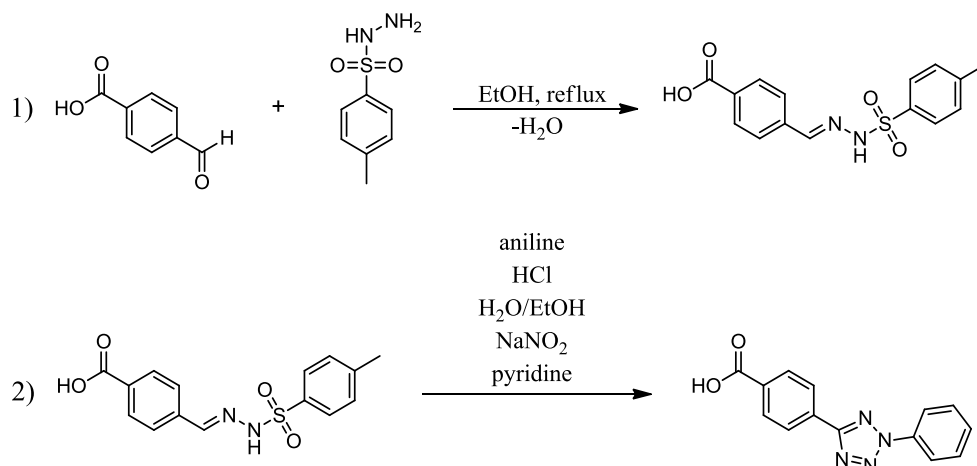
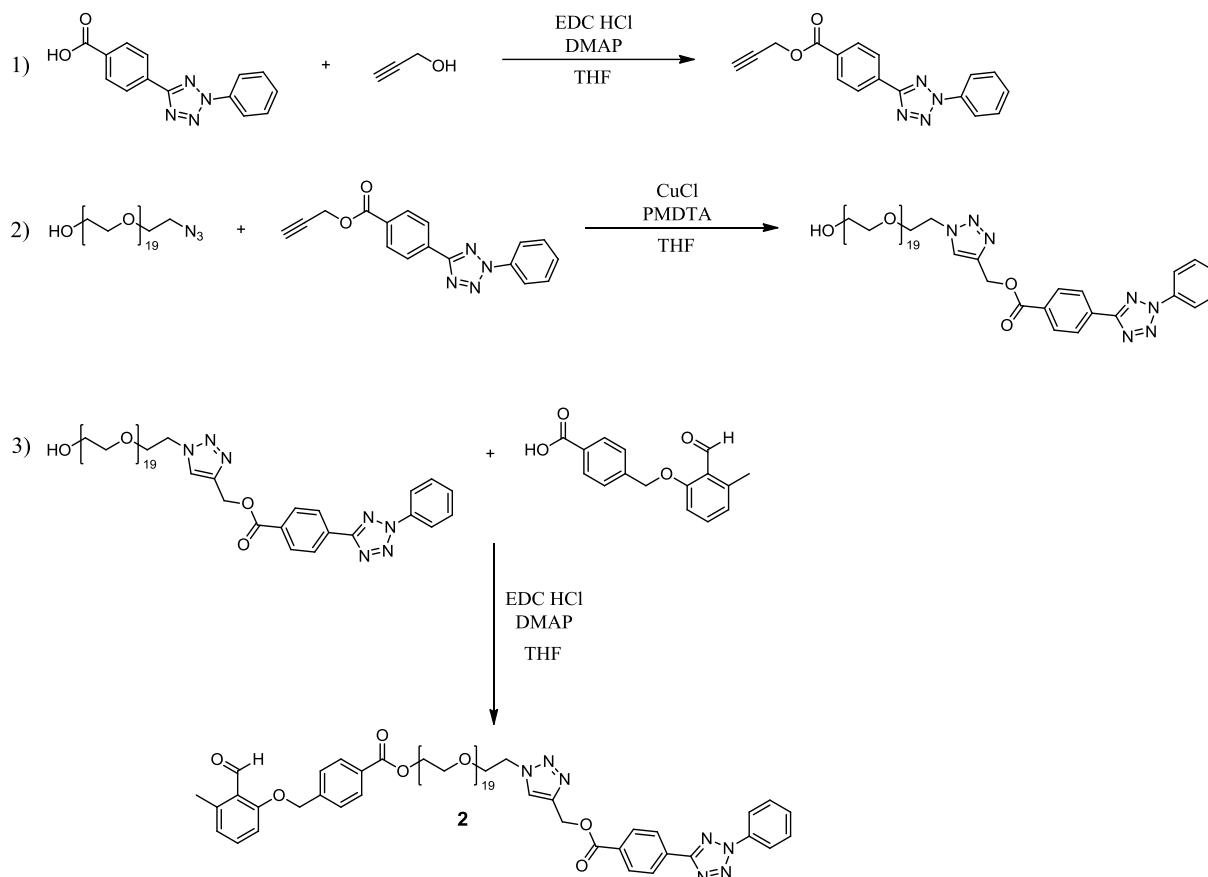


Figure S4. ¹H NMR of 4-((2-formyl-3-methylphenoxy)methyl) benzoic acid in DMSO-d₆.

4-(2-Phenyl-2H-tetrazol-5-yl) benzoic acid



α,ω -functional polymer 2



The synthesis of the α,ω -functional photoreactive polymer **2** was performed in three steps according to the appropriate literature procedure.^[5] The purity of **2** was confirmed by ¹H NMR, high resolution ESI-MS (Orbitrap), GPC, and UV/vis spectroscopy.

¹H NMR (CDCl₃) δ /ppm 2.52 (s, 3H), 3.35-3.70 (m, 72H), 3.77 (t, ³J = 5.2 Hz, 2H), 3.83 (t, ³J = 5.2 Hz, 2H), 4.41 (t, ³J = 5.2 Hz, 2H), 4.50 (t, ³J = 5.0 Hz, 2H), 5.16 (s, 2H), 5.45 (s, 2H), 6.76-6.83 (m, 1H), 7.26-7.33 (m, 1H), 7.39-7.57 (m, 7H), 7.86 (s, 1H), 7.99-8.07 (m, 2H), 8.11-8.17 (m, 4H), 8.26 (d, ³J = 8.8 Hz, 2H), 10.68 (s, 1H).

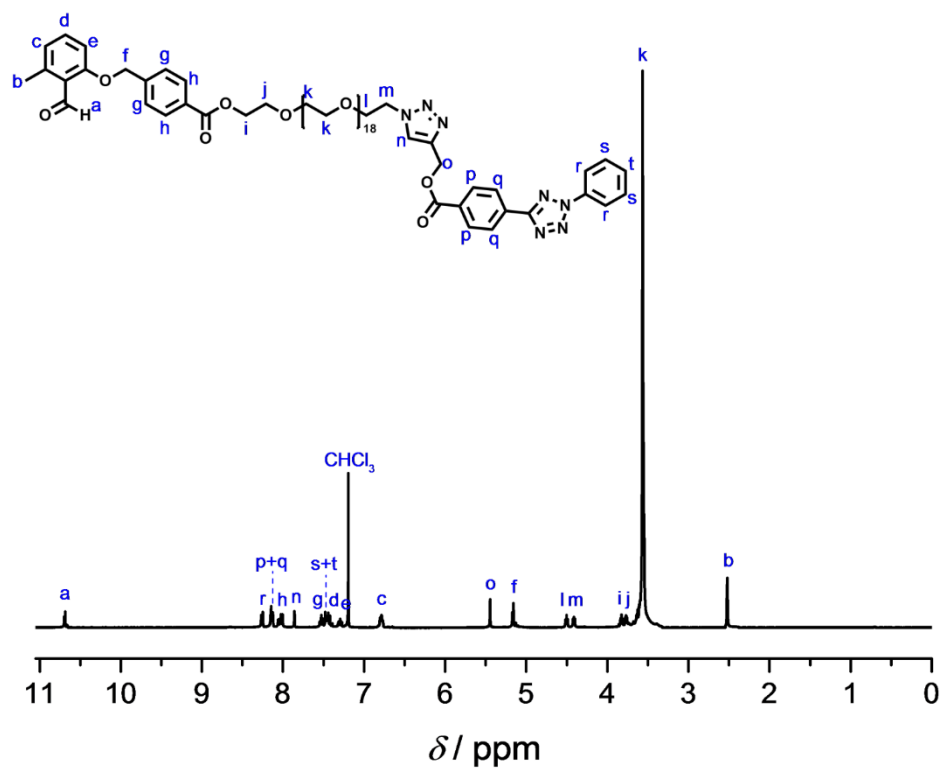


Figure S6. ^1H NMR of the α,ω -functional polymer **2** in CDCl_3 .

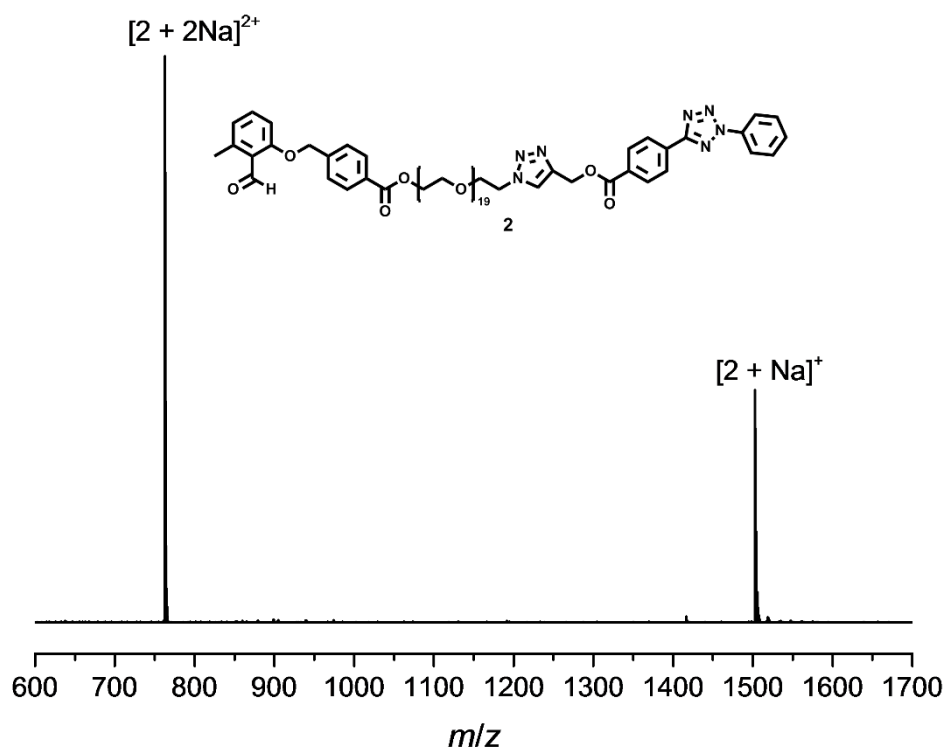


Figure S7. Orbitrap ESI-MS investigation of **2**.

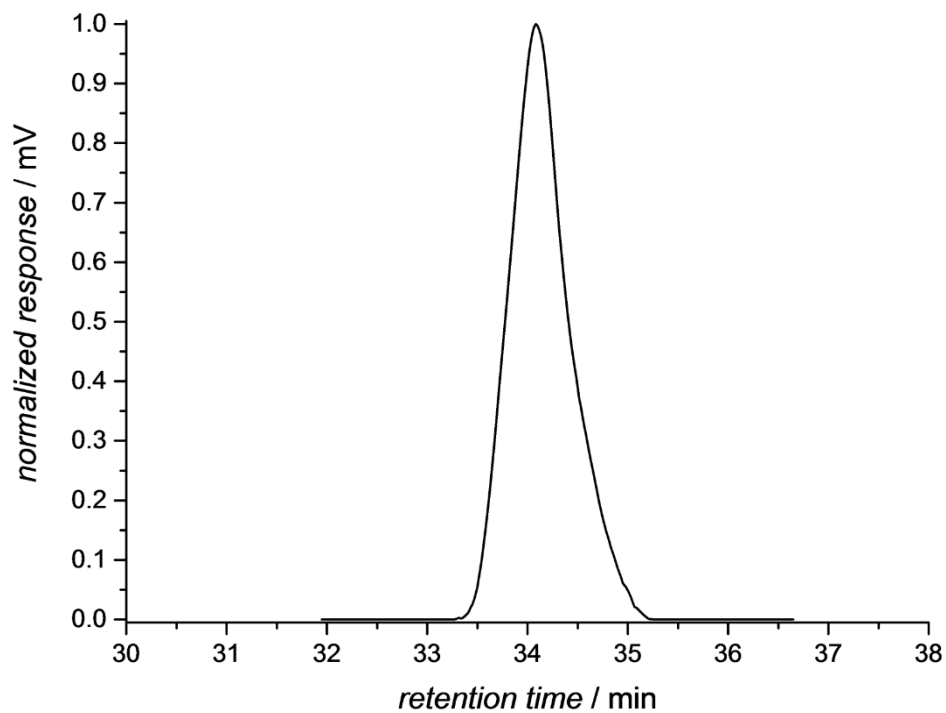


Figure S8. GPC trace of **2** in THF ($M_n = 1500$, $D = 1.04$)

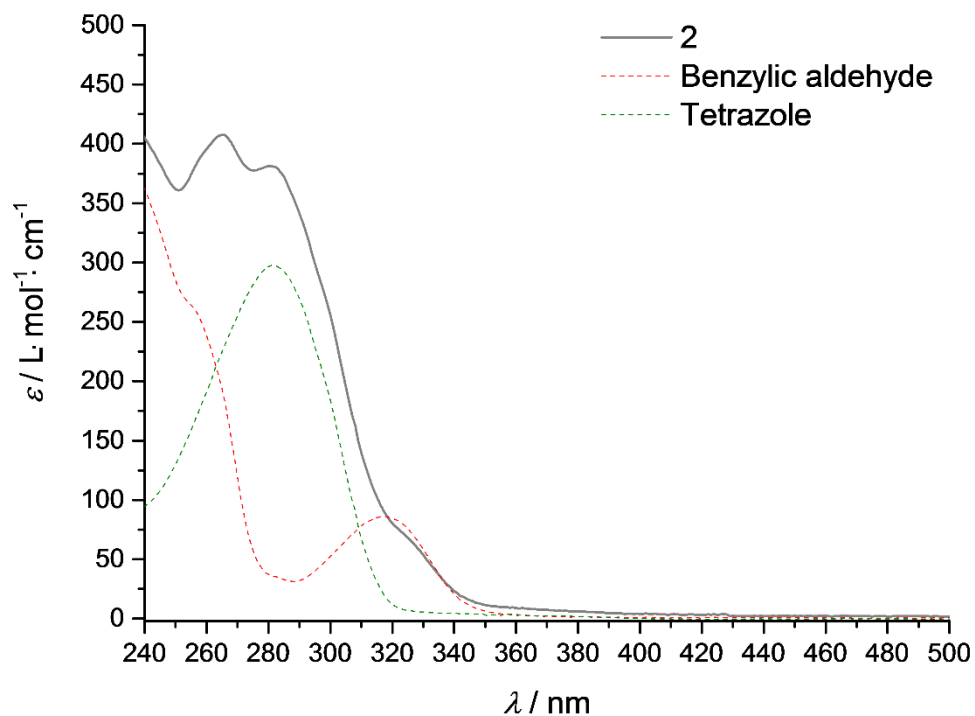
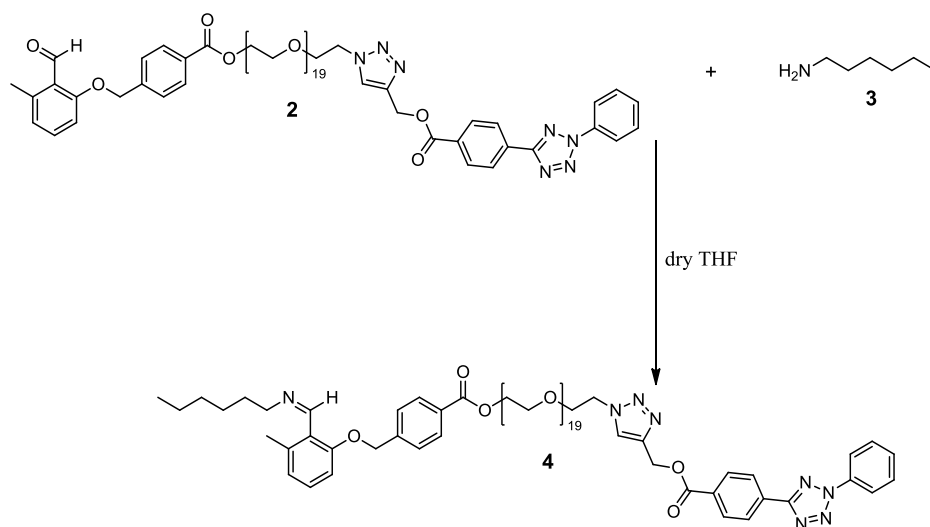


Figure S9. UV/vis spectrum of **2** in DCM ($c = 5 \cdot 10^{-3} \text{ mol} \cdot \text{L}^{-1}$, $d = 1 \text{ cm}$). The UV/vis spectra of benzaldehyde and tetrazole at identical concentrations are also shown on the graph.

Telechelic polymer-imine **4**



10.0 g (6.8 μmol , 1 eq.) of the α,ω -functional polymer **2** and 2.49 μL (18.9 mmol, 2.8 eq.) hexylamine were dissolved in 1.5 mL dry THF. The solution was stirred for 3 h at ambient temperature. The purity of **2** was confirmed by ^1H NMR, high resolution ESI-MS (orbitrap), and GPC.

^1H NMR (CDCl_3) δ/ppm 0.81 (t, $^3\text{J} = 7.0$ Hz, 2H), 1.14-1.38 (m, 6H), 1.63 (p, $^3\text{J} = 6.9$ Hz, 2H), 2.43 (s, 3H), 3.35-3.70 (m, 74H), 3.77 (t, $^3\text{J} = 5.0$ Hz, 2H), 3.83 (t, $^3\text{J} = 4.9$ Hz, 2H), 4.41 (t, $^3\text{J} = 4.8$ Hz, 2H), 4.50 (t, $^3\text{J} = 4.9$ Hz, 2H), 5.08 (s, 2H), 5.44 (s, 2H), 6.68 (d, $^3\text{J} = 8.4$ Hz, 1H), 6.78 (d, $^3\text{J} = 7.6$ Hz, 1H), 7.09 (t, $^3\text{J} = 8.0$ Hz, 1H), 7.37-7.56 (m, 6H), 7.86 (s, 1H), 7.99 (d, 2H), 8.11-8.17 (m, 4H), 8.26 (d, $^3\text{J} = 8.8$ Hz, 2H), 8.63 (s, 1H).

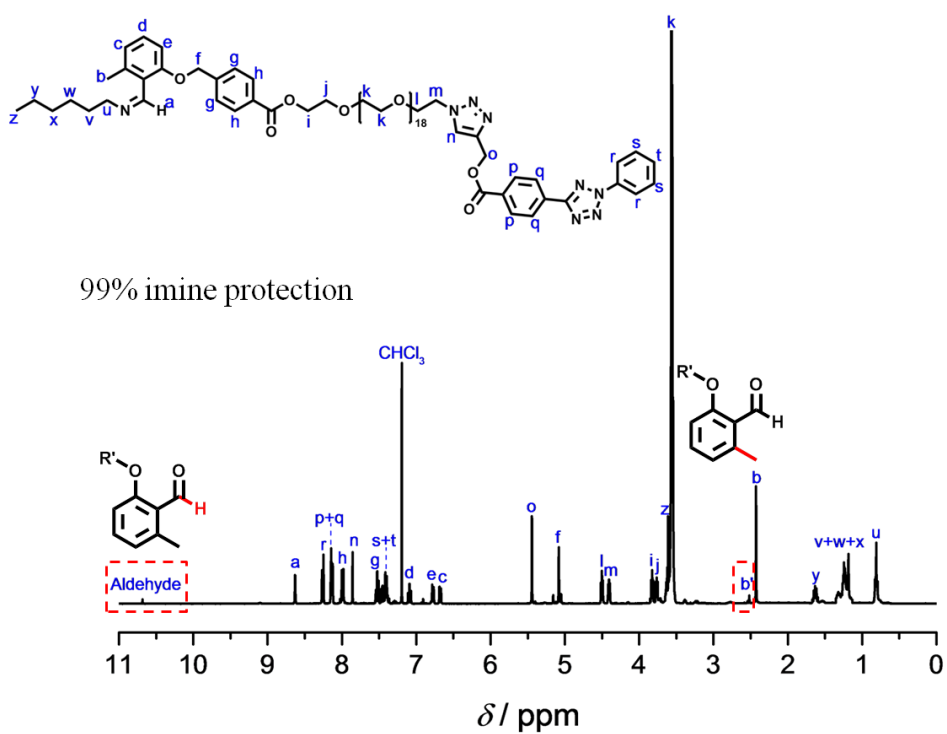


Figure S10. ^1H NMR of **4** in CDCl_3 .

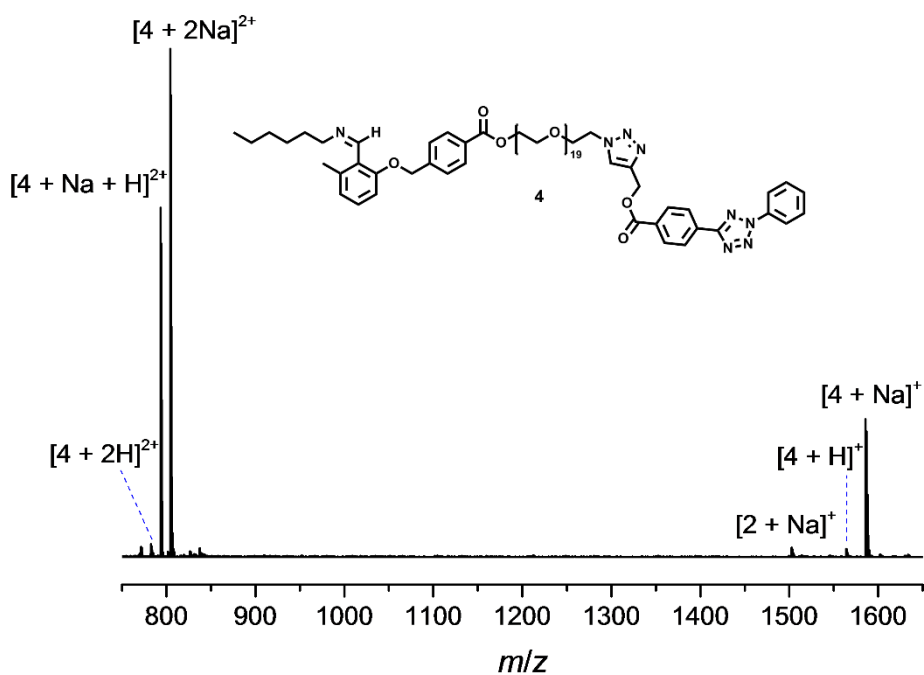


Figure S11. Orbitrap ESI-MS investigation of **4**. A residual amount (1 %) of the starting material **2** is detectable.

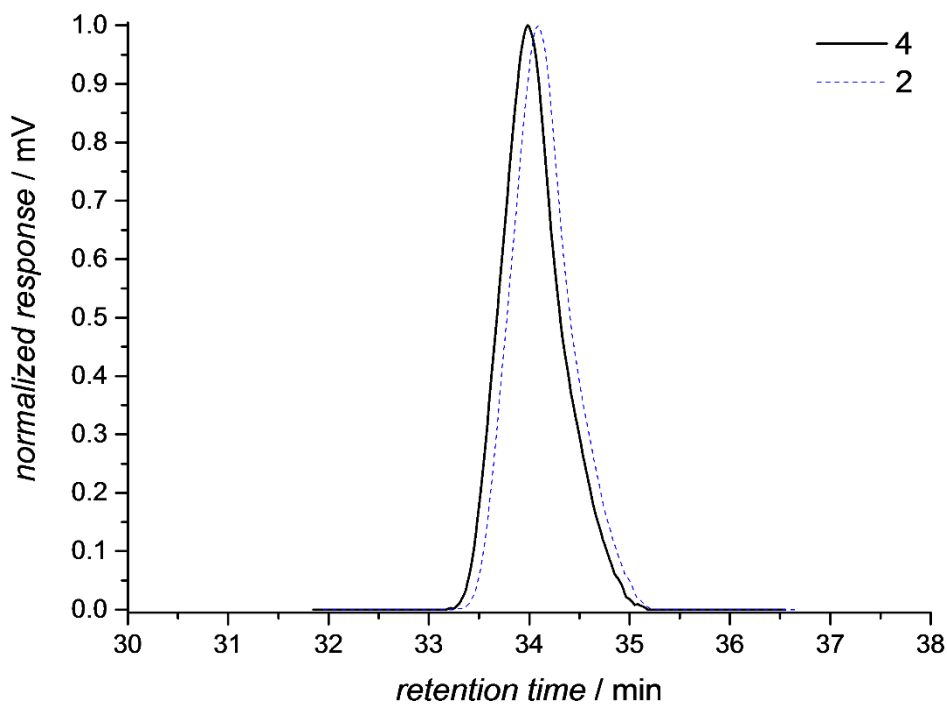


Figure S12. GPC trace of **4** in THF. A small shift towards higher molecular masses from the bilinker **2** in comparison to the bilinker imine **4** is detectable.

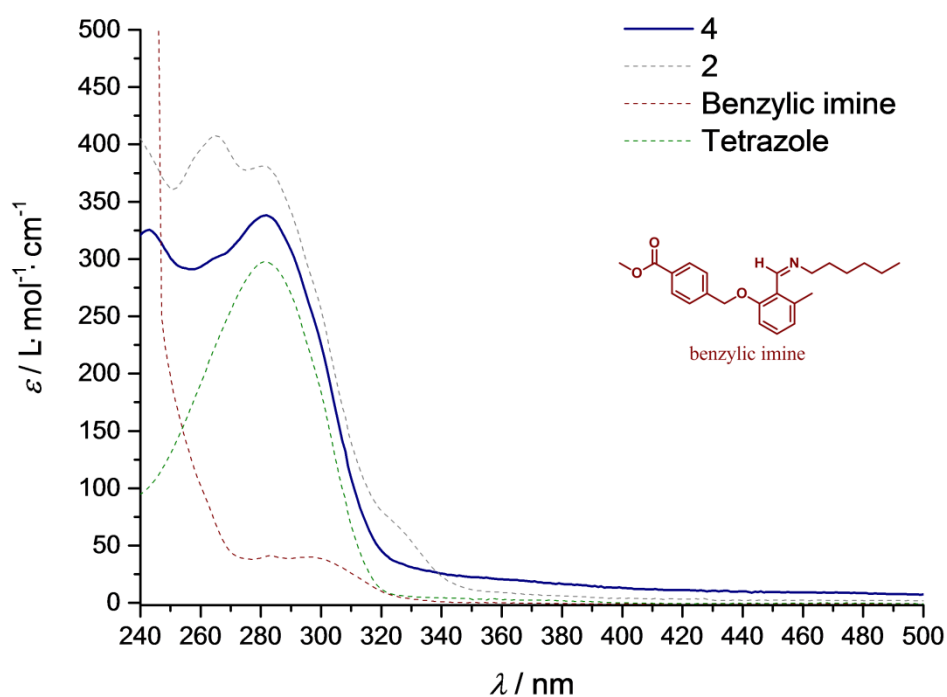
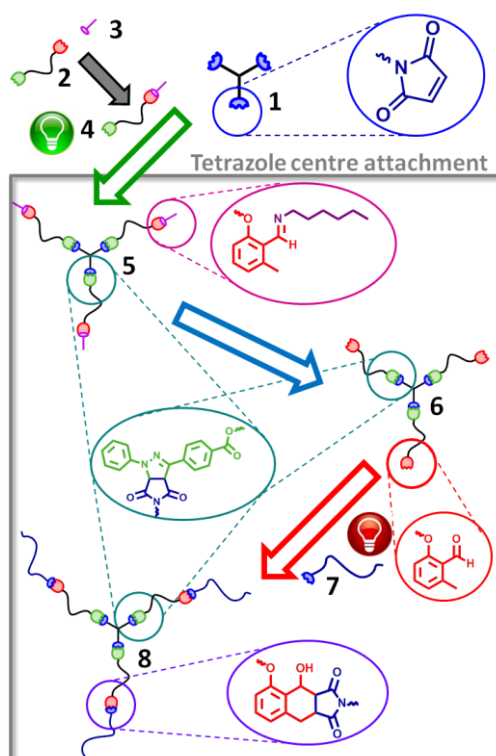
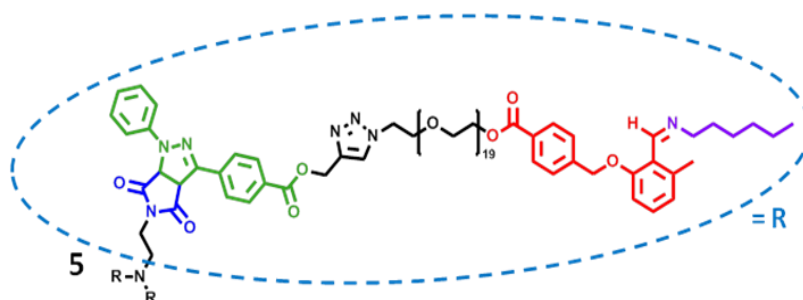


Figure S13. UV/vis spectroscopy of **4** in dichloromethane ($c = 5 \cdot 10^{-3} \text{ mol} \cdot \text{L}^{-1}$, $d = 1 \text{ cm}$). The UV/vis spectra of the bilinker **2**, a comparative benzylic imine and the tetrazole at an identical concentration are also shown on the graph.

Tetrazole core attached star polymer formation



Synthesis of **5**



$M = 4993.78 \text{ g}\cdot\text{mol}^{-1}$

0.5 mg (1.3 μmol , 1 eq.) of tris(2-maleimidoethyl)amine **1** and 6.1 mg (3.9 μmol , 3 eq.) of **4** were dissolved in 0.5 mL dry dichloromethane and separated into two aliquots in headspace vials (0.25 mL in each one, Pyrex, diameter 7 mm). The vials containing the solution were crimped air-tight using SBR seals with PTFE inner line. The solutions were then deoxygenated by purging the vials with nitrogen for 5 min. Both of the flasks were subsequently irradiated for 13 h by revolving around a compact low-pressure fluorescent lamp (Arimed B6, Cosmedico GmbH) emitting in the wavelength range of 280-440 nm. After the irradiation, the solvent was evaporated and the obtained polymer **5** was analyzed via ^1HMR and GPC.

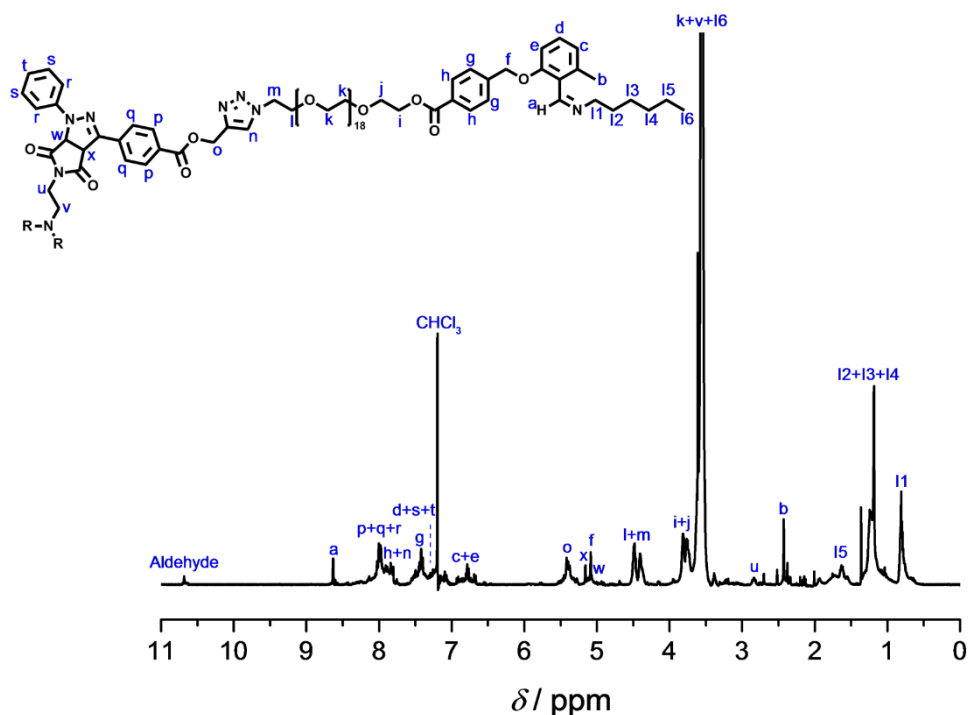
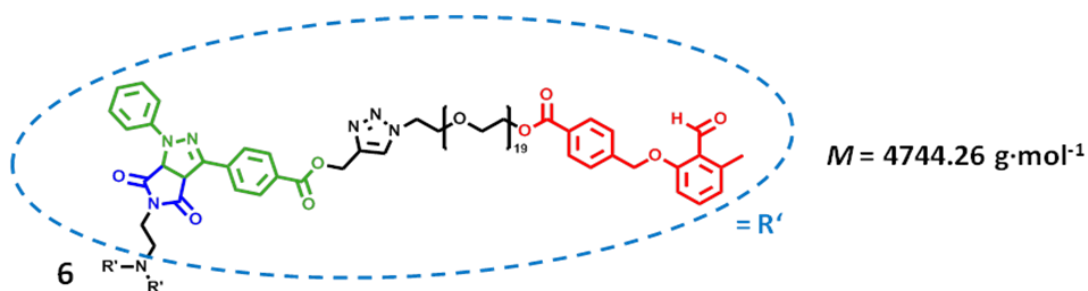


Figure S14. ^1H NMR of the imine terminated star shaped polymer **5** in CDCl_3 . The measurement proves the sole attachment of the tetrazole moiety of **4** to the maleimide core. A small amount of the photochemically inactivated imine was transformed into the benzaldehyde (5%). The Diels-Alder reaction between photoenol and maleimide is not detectable.

Synthesis of **6**



6.6 mg (4.2 μmol , 1 eq.) of **5** was dissolved in 2 mL THF containing wet molecular sieves (3 Å). The solution was left overnight at ambient temperature. After the imine deprotection the molecular sieves were removed and the solvent was subsequently evaporated under reduced pressure. The obtained polymer was analyzed via ^1H NMR and GPC.

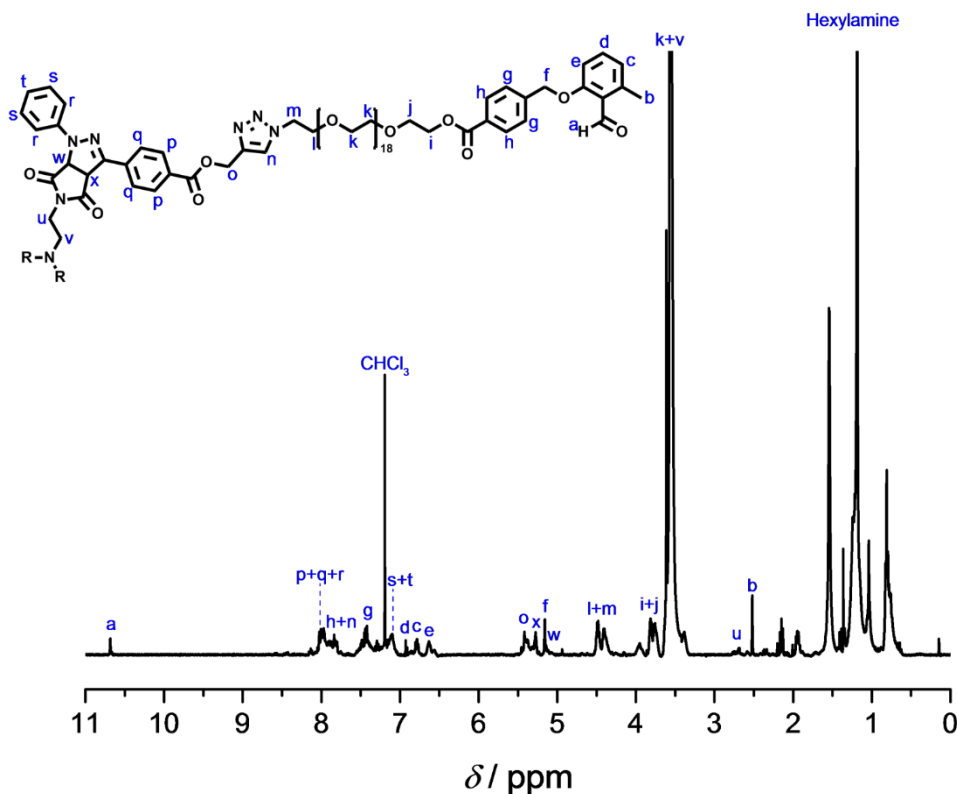
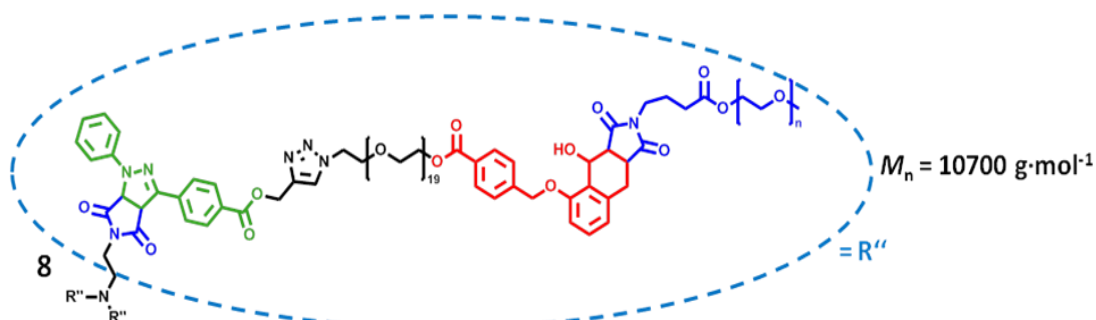


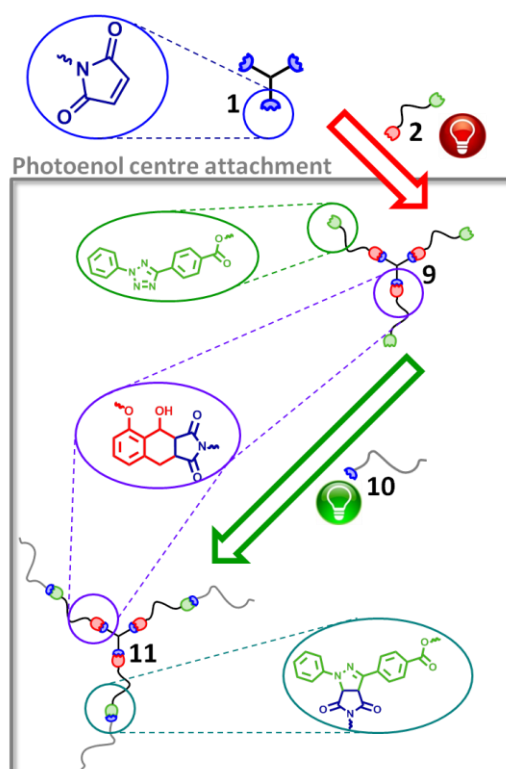
Figure S15. ^1H NMR of the benzaldehyde terminated star shaped polymer **6** in CDCl_3 . The measurement proves the complete imine transformation into the aldehyde form.

Synthesis of **8**

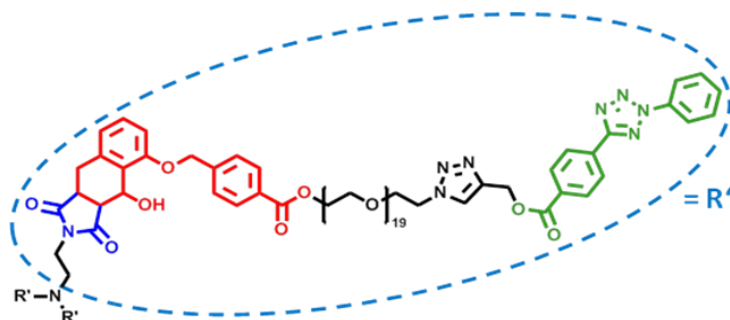


4.5 mg (0.9 μmol , 1 eq.) of the benzaldehyde terminated star shaped precursor **6** and 6.5 mg (2.8 μmol , 3 eq.) of PEG-maleimide **7** were dissolved in 1.0 mL dichloromethane and separated into two aliquots in headspace vials (0.5 mL in each one, Pyrex, diameter 7 mm). The vials containing the solution were crimped air-tight using SBR seals with PTFE inner line. The solutions were deoxygenated by purging the vials with nitrogen for 5 min. Both of the flasks were subsequently irradiated for 3 h by revolving around a compact low-pressure fluorescent lamp (PL-L, Philips Deutschland GmbH) emitting in the wavelength range of

Benzaldehyde core attached star polymer formation



Synthesis of **9**



$$M = 4828.30 \text{ g}\cdot\text{mol}^{-1}$$

0.6 mg (1.5 μmol , 1 eq.) of tris(2-maleimidoethyl)amine **1** and 6.9 mg (4.7 μmol , 3 eq.) of the bilinker **2** were dissolved in 0.5 mL dichloromethane and separated into two aliquots in headspace vials (0.25 mL in each one, Pyrex, diameter 7 mm). The vials containing the solution were crimped air-tight using SBR seals with PTFE inner line. The solutions were deoxygenated by purging the vials with nitrogen for 5 min. Both of the flasks were subsequently irradiated for 3 h by revolving around a compact low-pressure fluorescent lamp (PL-L, Philips Deutschland GmbH) emitting in the wavelength range of 300-440 nm. After the irradiation, the solvent was evaporated and the obtained polymer **8** was analyzed via ^1H NMR and GPC.

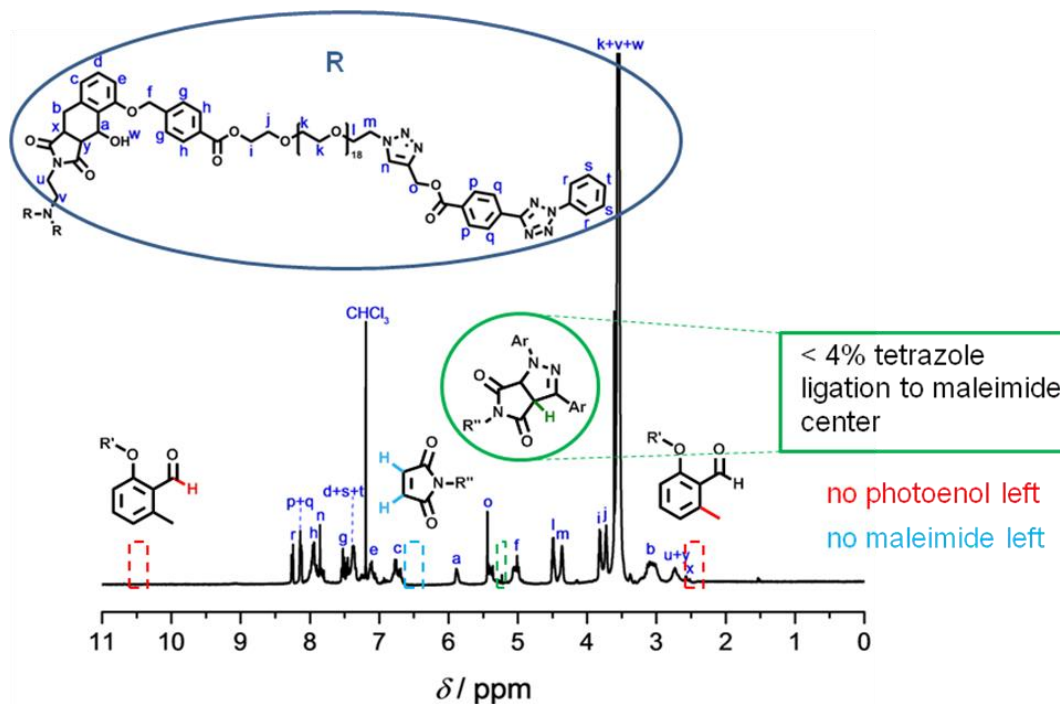
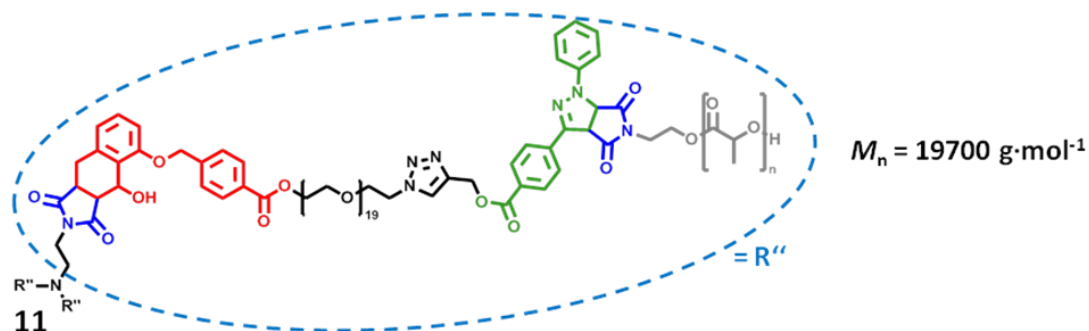


Figure S17. ^1H NMR of the tetrazole terminated star shaped polymer **9** in CDCl_3 .

Synthesis of **11**



2.5 mg ($0.5 \mu\text{mol}$, 1 eq.) of the tetrazole terminated star shaped precursor **9** and 8.1 mg ($1.5 \mu\text{mol}$, 3 eq.) of pL-maleimide **10** were dissolved in 1.0 mL dichloromethane and separated into two aliquots in headspace vials (0.5 mL in each one, Pyrex, diameter 7 mm). The vials containing the solution were crimped air-tight using SBR seals with PTFE inner line. The solutions were deoxygenated by purging the vials with nitrogen for 5 min. Both of the flasks were subsequently irradiated for 13 h by revolving around a compact low-pressure fluorescent lamp (Arimed B6, Cosmedico GmbH) emitting in the wavelength range of 280-440 nm.

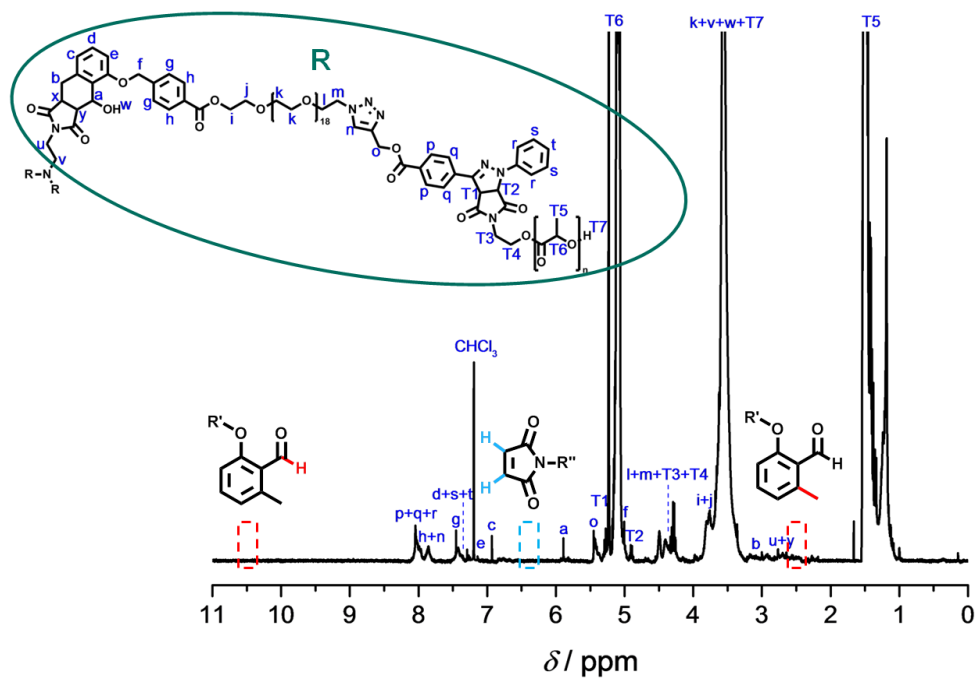
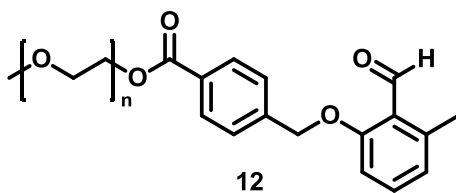


Figure S18. ^1H NMR of the pL terminated star shaped polymer **11** in CDCl_3 .

Benzaldehyde containing poly(ethylene glycol) 12



The synthesis of the benzaldehyde capped poly(ethylene glycol) **12** was performed according to a literature procedure.^[1] The end group fidelity was confirmed by ESI-MS (see ESI S21). The purity was confirmed by ¹H NMR (see ESI S20).

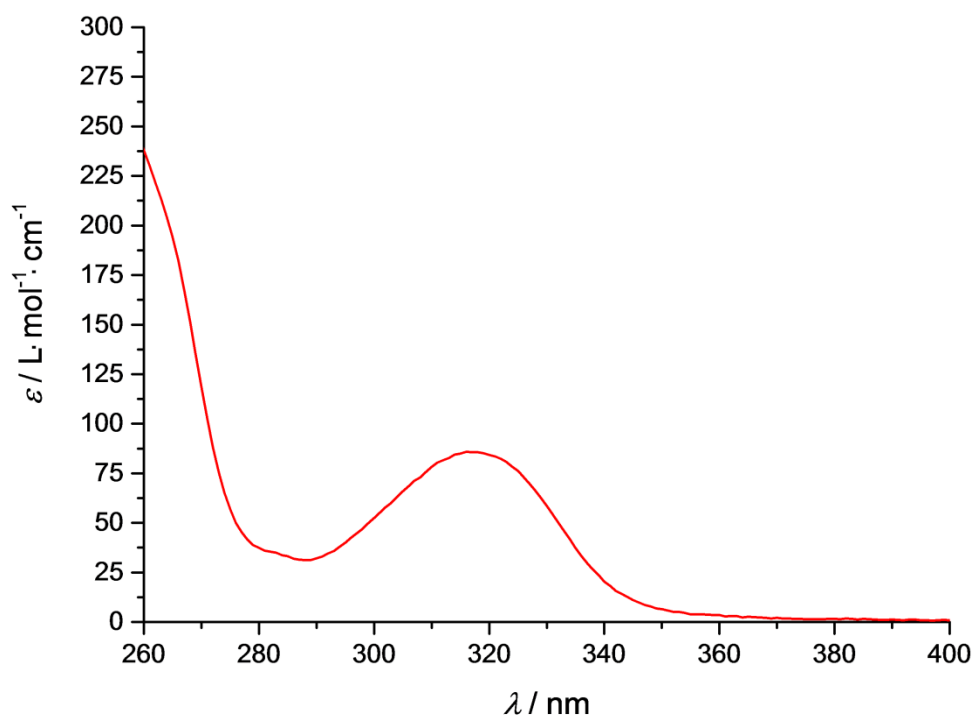


Figure S19. UV/vis spectrum of **1** ($c = 2 \cdot 10^{-3} \text{ mol} \cdot \text{L}^{-1}$, $d = 1 \text{ cm}$) in dichloromethane.

¹H NMR (CDCl₃) δ /ppm 2.52 (s, 3H), 3.31 (s, 3H), 3.42-3.74 (m, 200 H), 3.77 (t, ³J = 4.9 Hz, 2H), 4.41 (t, ³J = 4.8 Hz, 2H), 5.16 (s, 2H), 6.79 (t, ³J = 8.5 Hz, 2H), 7.29 (t, ³J = 8.5 Hz, 1H), 7.43 (d, ³J = 8.1 Hz, 2H), 8.02 (d, ³J = 8.3 Hz, 2H), 10.69 (s, 1H).

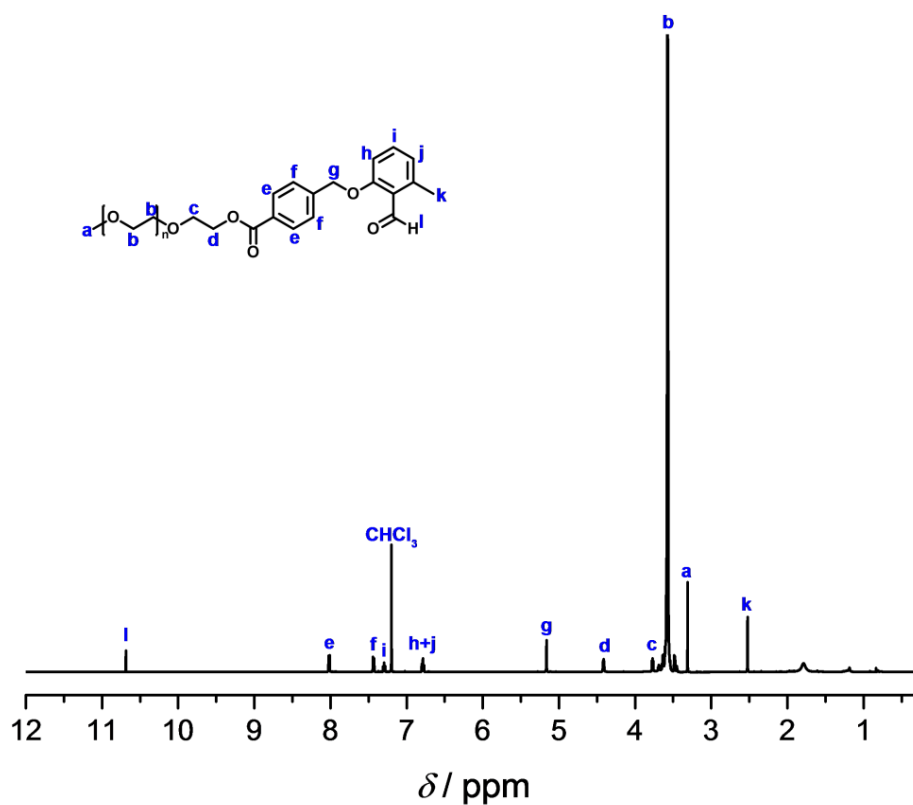


Figure S20. ^1H NMR of **12** in CDCl_3 .

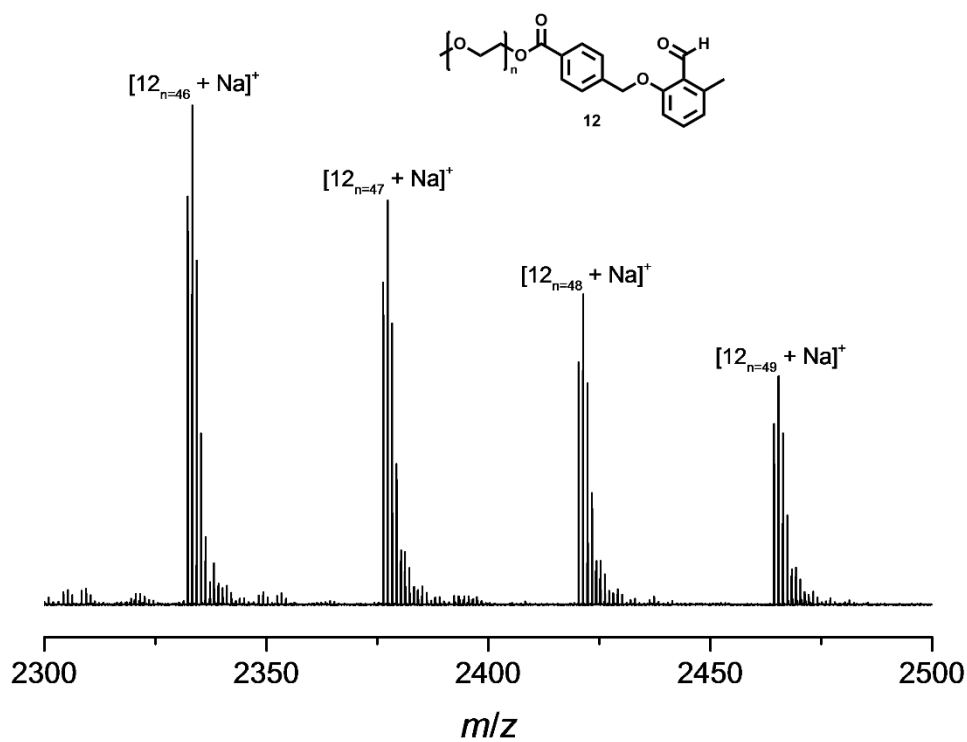
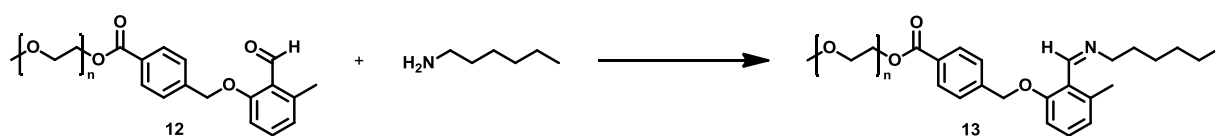


Figure S21. Expansion of the ESI-MS spectrum of **12**.

Evidencing the versatility of hexylamine as a protection group for photoreactions including 4-((2-formyl-3-methylphenoxy)methyl) benzoic acid (benzaldehyde)

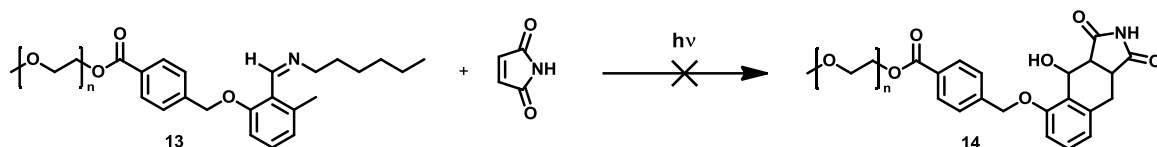
The transformation of the photoactive benzaldehyde **12** into the imine **13** leads to the temporarily photochemical deactivation of the compound. The removal of the imine functionality resulting in the re-formation of the aldehyde group reactivates the photoactive behaviour. The irradiation procedure of the benzaldehyde and the imine in the presence of maleimide is presented below:

A)



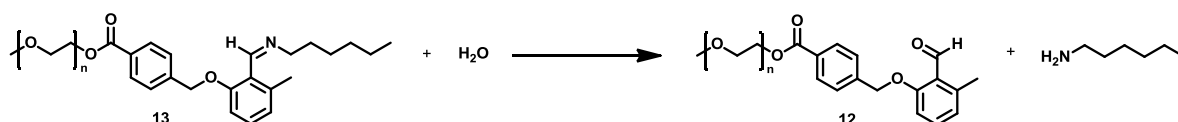
4.0 mg (1.4 μmol , 1 eq.) of the benzaldehyde terminated PEG **12** and 0.5 mg (5.1 μmol , 3.6 eq.) of hexylamine **3** were dissolved in 0.3 mL deuterated acetonitrile. The solution was left for 24 h and analyzed via ^1H NMR.

B)



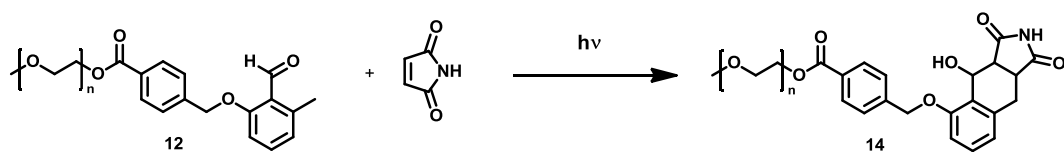
0.5 mg (5.5 μmol , 3.8 eq.) maleimide was added to the previous solution A. The solution was deoxygenated by purging the vials with argon for 5 min and irradiated subsequently for 30 min at $\lambda_{\text{max}} = 365$ nm using a Rayonet photoreactor. The inhibition of the light triggered Diels-Alder reaction due to the imine protection group was depicted by an *in-situ* ^1H NMR measurement.

C)



4.4 mg (222.0 μmol , 155.0 eq.) D_2O and 2.1 mg (35.0 μmol , 24.5 eq.) acetic acid were added to the previous solution B. The solution was left for 5 min and analyzed via ^1H NMR.

D)



The solution D was deoxygenated by purging the vials with argon for 5 min and irradiated subsequently for 60 min at $\lambda_{\text{max}} = 365$ nm using a Rayonet photoreactor. The *in-situ* light triggered Diels-Alder reaction of the benzaldehyde with maleimide was analyzed via ^1H NMR measurement.

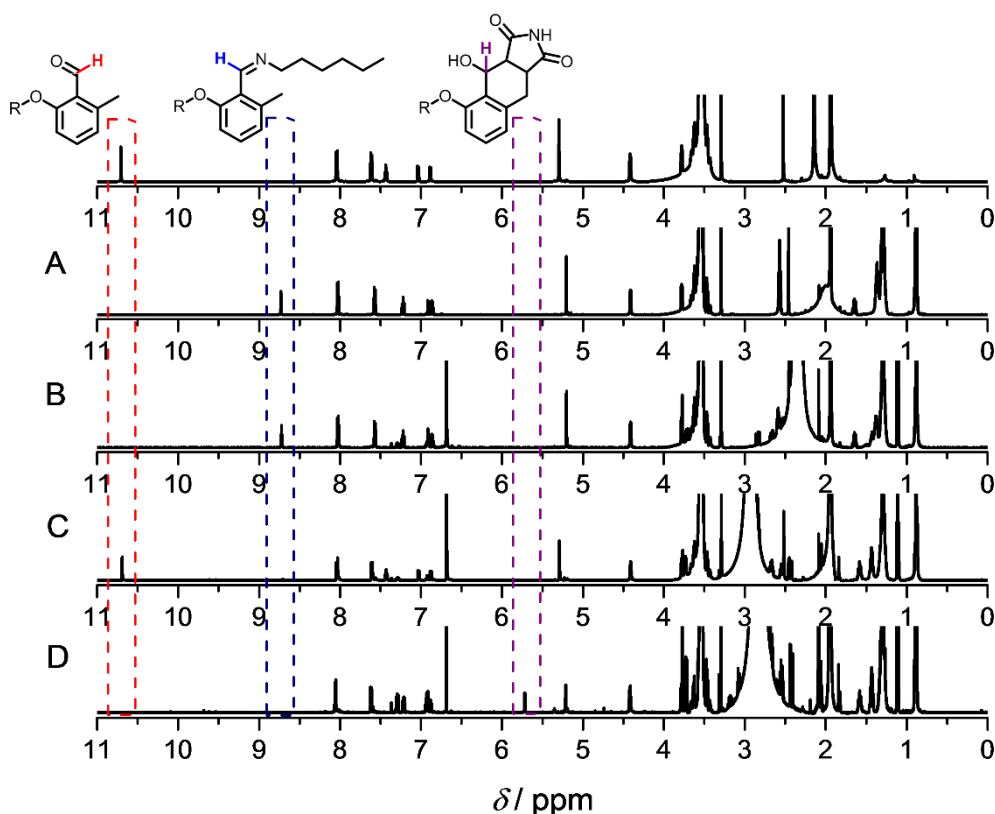


Figure S22. ^1H NMR analysis of the imine protection group during irradiation in CD_3CN . The aldehyde signal ($\delta = 10.71$ ppm) indicates the presence of the photoactive benzaldehyde **12** (top row). The imine transformation of the benzaldehyde with hexylamine yielding **13** is traced by the occurrence of the imine signal at $\delta = 8.72$ ppm (A). The irradiation of **13** with maleimide does not result in the Diels-Alder reaction. The imine signal ($\delta = 8.72$ ppm) remains unchanged (B). The hydrolysis of the imine **13** with D_2O and acetic acid results in the back formation of the photoactive aldehyde moiety, which can be traced by the presence of the aldehyde signal ($\delta = 10.71$ ppm) and the absence of the imine signal (D). The subsequent irradiation of the obtained benzaldehyde **12** leads to the formation of the Diels-Alder product

14, which can be verified by the ring formation ($\delta = 5.72$ ppm) and the absence of the aldehyde signal.

Theoretical and experimental values for all ESI-MS measurements

Table S1. Experimental and theoretical m/z values for the isotopic distributions of Figure S7 in the single and double charged m/z range between 600 and 1700.

m/z_{expt}	ion assignment	formula	m/z_{theor}	$\Delta m/z_{\text{expt}}$
762.8478	$[\mathbf{2} + 2\text{Na}]^{2+}$	$[\text{C}_{73}\text{H}_{105}\text{N}_7\text{Na}_2\text{O}_{25}]^{2+}$	762.8473	0.0005
1502.7068	$[\mathbf{2} + \text{Na}]^+$	$[\text{C}_{73}\text{H}_{1057}\text{NaO}_{25}]^+$	1502.7052	0.0016

Table S2. Experimental and theoretical m/z values for the isotopic distributions of Figure S11 in the single and double charged m/z range between 750 and 1650.

m/z_{expt}	ion assignment	formula	m/z_{theor}	$\Delta m/z_{\text{expt}}$
782.3926	$[\mathbf{4} + 2\text{H}]^{2+}$	$[\text{C}_{79}\text{H}_{120}\text{N}_8\text{O}_{24}]^{2+}$	782.4202	0.0276
793.4151	$[\mathbf{4} + \text{Na} + \text{H}]^{2+}$	$[\text{C}_{79}\text{H}_{119}\text{N}_8\text{NaO}_{24}]^{2+}$	793.4112	0.0039
804.4060	$[\mathbf{4} + 2\text{Na}]^{2+}$	$[\text{C}_{79}\text{H}_{118}\text{N}_8\text{Na}_2\text{O}_{24}]^{2+}$	804.4022	0.0038
1563.8417	$[\mathbf{4} + \text{H}]^+$	$[\text{C}_{79}\text{H}_{119}\text{N}_8\text{O}_{24}]^+$	1563.8332	0.0085
1585.8239	$[\mathbf{4} + \text{Na}]^+$	$[\text{C}_{79}\text{H}_{118}\text{N}_8\text{NaO}_{24}]^+$	1585.8152	0.0087

Table S3. Experimental and theoretical m/z values for product assignments relating to Figure S21 in the single charged m/z range between 2300 and 2500.

m/z_{expt}	ion assignment	formula	m/z_{theor}	$\Delta m/z_{\text{expt}}$
2332.3163	$[\mathbf{12}_{(n=46)} + \text{Na}]^+$	$[\text{C}_{109}\text{H}_{200}\text{NaO}_{50}]^+$	2332.3000	0.0163
2376.3428	$[\mathbf{12}_{(n=47)} + \text{Na}]^+$	$[\text{C}_{111}\text{H}_{204}\text{NaO}_{51}]^+$	2376.3262	0.0166
2420.3689	$[\mathbf{12}_{(n=48)} + \text{Na}]^+$	$[\text{C}_{113}\text{H}_{208}\text{NaO}_{52}]^+$	2420.3524	0.0165

References

- [1] T. Pauloehrl, G. Delaittre, V. Winkler, A. Welle, M. Bruns, H. G. Börner, A. M. Greiner, M. Bastmeyer, C. Barner-Kowollik, *Angew. Chem. Int. Ed.* **2012**, *51*, 1071-1074.
- [2] D. M. Bauer, A. Rogge, L. Stolzer, C. Barner-Kowollik, L. Fruk, *Chem. Comm.* **2013**, *49*, 8626-8628.

- [3] K. K. Oehlenschlaeger, J. O. Mueller, N. B. Heine, M. Glassner, N. K. Guimard, G. Delaittre, F. G. Schmidt, C. Barner-Kowollik, *Angew. Chem. Int. Ed.* **2013**, *52*, 762-766.
- [4] W. Song, Y. Wang, J. Qu, M. M. Madden, Q. Lin, *Angew. Chem. Int. Ed.* **2008**, *47*, 2832-2835.
- [5] K. Hildebrandt, T. Pauloehrl, J. P. Blinco, K. Linkert, H. G. Börner, C. Barner-Kowollik, *Angew. Chem. Int. Ed.* **2015**, *54*, 2838-2843.